



## **Abrasion prediction at Mud Mountain sediment bypass tunnel**

**Christian Auel, John R. Thene, Michelle Müller-Hagmann, Ismail Albayrak  
and Robert M. Boes**

### **Abstract**

A major drawback of sediment bypass tunnels is the potential for severe invert abrasion due to intense bedload sediment transport. This paper briefly describes the abrasion phenomena as well as the available models used to predict invert material loss. The application and calibration is demonstrated on the basis of the Mud Mountain sediment bypass tunnel, Washington, USA.

Keywords: abrasion rate, abrasion prediction model, granite pavement, invert wear

### **1 Introduction**

Dams interrupt continuous sediment transport along a river system leading to sediment accumulation in reservoirs. Hence, a sustainable use of reservoirs implies the application of strategies to counteract sedimentation. Mean annual sedimentation rates vary from 0.2% to some 2 to 3% of the reservoir volume with a global annual average rate of about 1%. Worldwide, increase in sedimentation volume exceeds increase in reservoir capacity revealing a gross storage loss (Schleiss and Oehy 2002, ICOLD 2009). Reservoir sedimentation has a number of negative effects. Firstly, lost volume in reservoirs leads to a loss of energy production, water used for water supply and irrigation, and retention volume (Annandale 2013). Secondly, operating safety is endangered due to blockage of outlet structures. Third, turbine abrasion due to increasing suspended sediment reduces efficiency and repair/replacement intervals. Finally, the trapping of sediment in a reservoir causes a sediment deficit in the tailwater that may result in downstream river incision, can destabilize river banks and may inhibit its ecologic connectivity (ICOLD 2009, Kondolf *et al.* 2014).

Managing sediment to minimize aggradation in reservoirs employs a variety of techniques categorized in three main countermeasures: (1) sediment yield reduction, (2) routing sediments around or through the reservoir, and (3) Sediment removal or dam heightening (e.g., Morris and Fan 1998, ICOLD 2009, Annandale 2013, Kondolf *et al.* 2014). In general, sediment routing is ecologically favorable compared to other measures as it is conducted during high flows when sediment load is already high. River bed erosion downstream of the dam can be slowed resulting in a recovery of morpho-

logical variability (Fukuda *et al.* 2012, Facchini *et al.* 2015, Martín *et al.* 2015, Auel *et al.* 2017a).

Moreover, only sediments delivered upstream of the bypass are diverted and the sediment concentration downstream of the dam is (almost) not affected and the river keeps its natural character (ICOLD 2009).

## **2 Advantages and disadvantages of sediment bypass tunnels**

Sediment routing using a bypass tunnel (SBT) is an effective strategy for both bed and suspended sediment loads (Sumi *et al.* 2004, Auel *et al.* 2016a). If all sediments are guided into the tunnel intake using guiding structures such as cofferdams, walls or weirs, the reservoir is kept free of sediments downstream of the intake. However, if the tunnel design discharge is exceeded, a partial flow will enter the reservoir bringing suspended load with it (Auel and Boes 2011).

The number of SBTs at reservoirs is limited with only about 30 worldwide. Most SBTs exist in Switzerland (Egschi, Hintersand, Palagnedra, Pfaffensprung, Rempen, Runcahez, Sera, Solis, Ual da Mulin, Val d'Ambra), Japan (Asahi, Koshibu, Matsukawa, Miwa, Nunobiki), and several in China and South Africa. Three SBT are under construction in Taiwan (Nanhua, Shimen, Tsengwen). Additionally, several flood bypass tunnels which perform similarly to SBTs operate in Switzerland and Japan (Auel *et al.* 2016a).

In general, SBT are operated in supercritical free-surface flow conditions, although some are operated under pressure for limited periods. Intakes are located either at the (1) reservoir head or (2) inside the reservoir. The first location results in long tunnels, but operation is simple and the entire reservoir can be kept free from sediment deposition. The second location allows for short tunnels, but both construction and operation are challenging. The reservoir must be lowered to the intake elevation prior to a flood event to allow for sufficient transport capacity towards the tunnel intake.

SBTs are highly effective at keeping the reservoir free of sediments. Research on the Japanese SBT Asahi and Nunobiki showed that on average, 77% and 94% of the incoming sediments were diverted to the downstream river reach, and the estimated reservoir life was prolonged to 450 and 1200 years, respectively (Auel *et al.* 2016a). SBTs also improve the ecological function in rivers by connecting the up- and downstream reaches in terms of sediment continuity. The natural morphological river characteristics are thereby reestablished, and microhabitat and invertebrate richness in the downstream reaches are equal to the upstream values (Auel *et al.* 2017a).

The high construction cost of SBTs has limited their use to small and medium-sized reservoirs ( $<10^7$  m<sup>3</sup>) where tunnel lengths are smaller and cost less. Another disadvantage is that floods up to the SBT design discharge are directly diverted into the tailwater with no retention. Therefore, SBTs are more common in regions with high

floods, whereas in arid regions the priority is to retain as much of the flood volume as possible.

Due to high bedload sediment transport with grain sizes in the decimeter range, many SBT face severe invert abrasion (Jacobs *et al.* 2001, Auel and Boes 2011, Boes *et al.* 2014, Baumer and Radogna 2015). These tunnels, however, operate effectively despite significant abrasion. These abrasion problems cause high periodical maintenance costs, inhibiting implementation of new SBTs.

### 3 Abrasion

Abrasion is a wear phenomenon involving progressive material loss due to hard particles forced against and moving along a solid surface controlled by kinetic energy due the vertical component of a saltating particle impact (deformation wear), and friction due to grinding stress (cutting wear) caused by the horizontal component (Bitter 1963a, b). In general, abrasive damage can always be expected when particle bedload transport takes place. The governing process causing abrasion on brittle materials such as bedrock and concrete is saltation, whereas sliding and rolling do not cause significant wear (Whipple *et al.* 2000, Sklar and Dietrich 2004; Turowski 2012; Beer and Turowski 2015).

The extent of damages along the wetted perimeter, i.e. mainly on the invert and the lower parts of the tunnel walls, typically increases with increasing sediment load, particle size as well as quartz content in the mineralogical composition of the sediments (Boes *et al.* 2014).

Several mechanistic models exist to predict abrasion rates. While the models for the prediction of bedrock incision (e.g., Sklar and Dietrich 2004, Lamb *et al.* 2008) focus on typical flow conditions in river systems in the sub- and low supercritical flow regimes, the others for prediction of abrasion on concrete surfaces (Ishibashi 1983, Helbig and Horlacher 2007, Auel *et al.* 2017b, c) have to account for highly supercritical flows. All models take the physical process of particle impact into account and are derived from experimental research on particle motion characteristics, i.e. the analysis of particle impacts, velocities and saltation trajectories.

The first published mechanistic model to determine concrete and steel abrasion on hydraulic structure surfaces was proposed by Ishibashi (1983). The abraded invert volume  $V_a$  is calculated as:

$$V_a = C_1 E_k + C_2 W_f \quad [1]$$

where  $E_k$  = total particle kinetic energy of saltating particles,  $W_f$  = total friction work by grinding particles, and  $C_1$  and  $C_2$  = invert material property constants for either concrete or steel. The total kinetic energy  $E_k$  is given by:

$$E_k = 1.5V_{ts} \sum E_i N_i n_i \text{ [kgf m]} \quad [2]$$

and the total friction work  $W_f$  by:

$$W_f = 5.513\mu_s V_{ts} \sum \left( \frac{U_p}{W_{im}} \right) E_i N_i n_i \text{ [kgf m]} \quad [3]$$

where  $V_{ts}$  = amount of transported sediment [ $\text{m}^3$ ],  $\mu_s$  = dynamic friction coefficient,  $E_i$  = kinetic energy of a single particle,  $U_p$  = horizontal particle velocity,  $W_{im}$  = vertical particle impact velocity,  $N_i = L/L_p$  = impact frequency, with  $L$  = total invert length and  $L_p$  = particle saltation length, and  $n_i$  = amount of particles per sediment volume. A detailed step by step calculation procedure is given in Auel *et al.* (2016b). Re-evaluation of Eq. (1) using long-term invert abrasion data of the Japanese SBT Asahi led to the conclusion that the second term in Eq. (1) ( $C_2 W_f$ ) should be dropped in case of concrete inverts (Auel *et al.* 2016b).

A widely applied model for bedrock incision was proposed by Sklar and Dietrich (2004) and follows in its general form:

$$A_r = \frac{Y_M}{k_v f_t^2} \cdot \frac{W_{im}^2}{L_p} \cdot q_s \cdot \left( 1 - \frac{q_s}{q_s^*} \right) \text{ [m/s]} \quad [4]$$

where  $Y_M$  = Young's Modulus of elasticity of the bed material [Pa],  $f_t$  = splitting tensile strength of the bed material [Pa],  $k_v = 10^6$  = non-dimensional abrasion coefficient encompassing both the particle and bed material characteristics,  $q_s$  = bed load mass transport rate per unit width [ $\text{kg}/(\text{sm})$ ], and  $q_s^*$  = bed load mass transport capacity per unit width [ $\text{kg}/(\text{sm})$ ]. The last term on the right of Eq. (4) is related to the cover effect accounting for bed load partly covering the bed (e.g., Sklar and Dietrich, 1998; Turowski, 2009). Sklar and Dietrich (2004) applied correlations of hop length, hop height and particle velocity for a wide data range to Eq. (4) and proposed the saltation abrasion model for bedrock river abrasion as:

$$A_r = 0.08g(s-1) \frac{Y_M}{k_v f_t^2} \cdot q_s \cdot \left( 1 - \frac{q_s}{q_s^*} \right) \left( \frac{\theta}{\theta_c} - 1 \right)^{-0.5} \left( 1 - \left( \frac{U_*}{V_s} \right)^2 \right)^{1.5} \text{ [m/s]} \quad [5]$$

where  $U_* = (gR_h S)^{0.5}$  = friction velocity,  $R_h$  = hydraulic radius,  $S$  = energy line slope for steady but gradually-varied flow, or bed slope for uniform flow,  $V_s$  = particle settling velocity,  $\theta$  = Shields parameter calculated as  $\theta = U_*^2 / [(s-1)gD]$ ,  $s = \rho_s / \rho$  with  $\rho_s$  = particle density and  $\rho$  = fluid density,  $D$  = particle diameter,  $\theta_c$  = critical Shields parameter. The last term in Eq. (5) accounts for the mode shift from saltation to suspension using a nonlinear function additionally increasing the hop length.

Auel *et al.* (2017c) proposed a revised version based on Eq. (4) accounting for sub- and supercritical flows as well as fixed planar and alluvial beds:

$$A_r = \frac{Y_M}{k_v f_t^2} \cdot \frac{(s-1)g}{230} q_s \left( 1 - \frac{q_s}{q_s^*} \right) \text{ [m/s]} \quad [6]$$

Based on similarity between bedrock and concrete (both being brittle materials), a material strength-dependent Young's modulus formulation as well as a correlation of compression to tensile strength were introduced (Auel *et al.* 2017c). Both, the Young's modulus reformulation and new equations for vertical impact velocity and hop length have led to a variation of the abrasion coefficient with  $k_v = 10^5$ , an order of magnitude lower than the values used by Sklar and Dietrich (2004).

## 4 Mud Mountain SBT

### 4.1 General information and background

Mud Mountain dam is a 132 m high flood retention dam, completed in 1948 and operated by the U.S. Army Corps of Engineers, Seattle District (Figure 1a). The dam impounds the White River during floods, a gravel bed river originating from the northern slope of Mt. Rainier, a 4.392 m high volcano in western Washington State, USA. The following data are summarized from Czuba *et al.* (2012), USACE (2016) and VAW (2016).

Two tunnels, 23 feet (7.0 m) and 9 feet (2.74 m) wide, drain the reservoir. The intake invert level of the 9-foot tunnel is at approx. 271 m a.s.l., while the 23-foot tunnel intake is at a higher elevation (Figure 1b). The maximum reservoir level is at 370 m a.s.l. defined by the spillway crest.

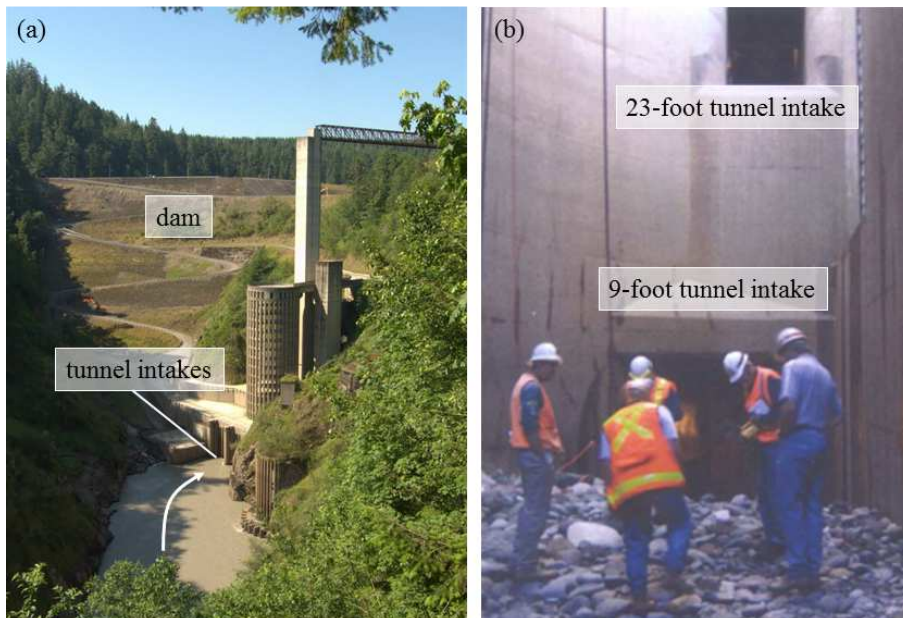


Figure 1: a) Photograph of Mud Mountain dam and tunnel intake structures in 2012 (courtesy of Mike Betz), b) photograph of tunnel intakes with gravel deposition (USACE 2016).

The 9-foot tunnel intake is pressurized, but shifts to supercritical open-channel flow downstream the gate which is opened almost the entire year diverting the White River into the tailwater. During floods, the 9-foot tunnel is operated for reservoir levels up to 283.5 m a.s.l. The tunnel is closed at higher reservoir levels and the 23-foot tunnel is then used to bypass incoming floods. Consequently, all bedload sediments are diverted through the 9-foot tunnel (termed SBT hereafter) while only suspended sediment laden water is diverted through the 23-foot tunnel. The SBT is 505 m long, the invert slope is  $S_b = 0.0194$ , and the cross section of archway type. The invert was lined with a 2.5 cm thick planar steel lining in 1995 extending vertically to the side walls.

The annual total sediment load entering the reservoir is about 450'000 tons while the bedload has a share of 11%, hence  $Q_s = 49,500$  tons/year with a variation of  $\pm 62\%$  representing wet years with many floods and dry years with rather low flow conditions, respectively. The median particle diameter is  $D_{50} = 62$  mm. The sediment loads have proven to be quite destructive. Major invert abrasion has been observed in the steel lining which was worn through in places after 12 years (Figure 2a). Several decimeter deep incision channels along the side walls developed within the underlying concrete foundation that was washed out. Furthermore, randomly distributed scour holes and longitudinal incision channels occurred where the steel lining was completely removed (Figure 2b).

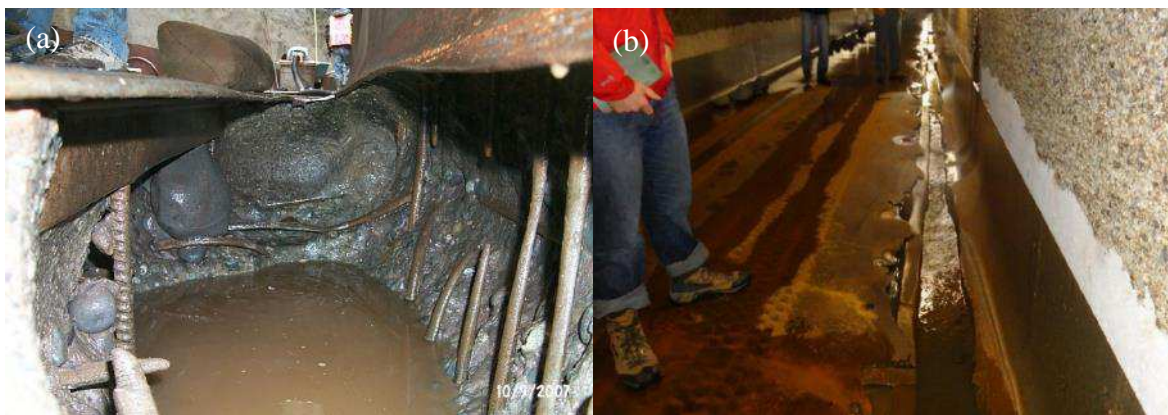


Figure 2: Abrasion patterns in the steel lining of Mud Mountain SBT, a) photograph in 2007: damage expanded into the concrete proof lining below the steel plate, b) photograph in 2015: longitudinal abrasion channel along the side wall (USACE 2016).

The US Army Corps of Engineers tendered the rehabilitation of the tunnel invert which was awarded to and is currently carried out by a joint venture of ILF Consulting Engineers and Garney Construction. As the preceding steel lining did not show adequate durability and service life, a granite invert consisting of rectangular-cut, 0.25 m thick natural stone pavers ( $0.6 \text{ m}^2$  and  $0.8 \text{ m}^2$ ) was proposed. A similar lining has been recently implemented at Pfaffensprung SBT, Switzerland (Müller and Walker, 2015). In the following, the future abrasion rate and depth of the invert lining of Mud Mountain SBT

is predicted for a range of hydraulic and bedload transport conditions by applying the above presented formulae (Eqs. 1, 5, 6).

## 4.2 Abrasion prediction

Calculations were performed based on the data given in USCE (2016). The flow depths  $h$  and velocities  $U$  were calculated for the existing SBT dimensions for three different discharges, i.e. low, medium (subscript  $med$ ) and the pool limit (subscript  $pl$ ) for the SBT at 283.5 m a.s.l. The newly proposed granite invert would decrease the net flow area of the tunnel cross section, leading to slight changes in these hydraulic parameters, i.e. slightly smaller flow depths and larger velocities. Sediment transport took place only on 83 out of 365 days (23%) in 2011 (VAW 2016). Hence, we concluded that bedload transport is only expected for river discharges  $Q > Q_{med}$ , which was exceeded during 20% of the year. Open-channel flow conditions in the tunnel are non-uniform (steady, accelerated) and shift from pressurized flow to open-channel flow along the tunnel for  $Q_{med}$ , while they are completely pressurized for  $Q_{pl}$ . For sake of simplicity, we calculated the abrasion rates applying the average flow conditions (average of up- and downstream values). The bed slope  $S_b$  was applied to compute the friction velocity  $U_*$ , hence uniform flow was assumed. Hydraulic parameters are summarized in Table 1.

Table 1: Hydraulic parameters of Mud Mountain SBT

	$Q$ [m <sup>3</sup> /s]	$H^*$ [m]	$h$ [m]	$U$ [m/s]	Froude number [-]	Flow type
$Q_{med}$	56.6	7.38	2.36	9.3	1.9	Open-channel
$Q_{pl}$	68.0	11.95	2.50	11.3	-	Pressurized

\* Head at intake

The invert is planned to be lined with *Hardy Island granite* pavers with a material density of  $\rho_m = 2684 \text{ kg/m}^3$ , a compressive strength of  $f_c = 223 \text{ MPa}$ , a tensile strength of  $f_t = 11.7 \text{ MPa}$  and a Young's modulus of  $Y_M = 6.49 \times 10^4 \text{ MPa}$  (VAW 2016). Both tensile strength and Young's modulus were obtained from formulae given in Auel *et al.* (2017c).

A mean sediment load of 49,500 tons/year was assumed, while taking the hydrological variability into account by  $\pm 62\%$  of the sediment transport rate. The cover effect (Eqs. 5 and 6) was neglected as flows were supercritical and hence  $q_s^* \gg q_s$  (VAW 2016).

Table 2 summarizes the estimated mean (spatially averaged) abrasion rates  $A_r$  and the mean annual abrasion depths  $A_d$  of Hardy Island Granite. The  $k_v$  values applied originate from both literature recommendations and a field calibration of the models based on Pfaffensprung SBT abrasion data (VAW 2016, Müller-Hagmann 2017). Considering granite, the literature recommendations may yield unrealistically high estimates. Abra-

sion estimation for the granite invert at Pfaffensprung SBT with the Auel and the Sklar and Dietrich models using the literature  $k_v$  values significantly overestimated the measured abrasion depths from 2012 to 2014 (Müller-Hagmann 2017). Hence, the Pfaffensprung calibrated  $k_v$  values were also applied for Mud Mountain (columns 5-8 in Table 2).

Moreover, two scenarios were distinguished: (1) a more likely scenario with average abrasion condition ( $k_v$  value determined from the total abrasion depth over three years of Pfaffensprung SBT operation) and (2) rare scenario with severe abrasion conditions (minimum  $k_v$  value determined from the highest measured annual abrasion depth within three years of Pfaffensprung SBT operation). For the Ishibashi model, only a mean scenario was applied.

Table 2: Spatially averaged abrasion rates  $A_r$  and annual abrasion depths  $A_d$  predicted using different prediction models

Model	Literature			Pfaffensprung field data calibration				
	Auel	Sklar and Dietrich	Ishibashi	Auel	Sklar and Dietrich	Ishibashi		
Equations	[6]	[5]	[1]	[6]	[5]	[1]		
Abrasion scenario				severe	average	severe	average	average*
$k_v$ value [ $10^6$ ]	0.1	1.0		1.2	1.65	7.0	12.5	-
$C_l$ [ $10^{-7}$ m <sup>2</sup> /(kgf)]			1.189					0.0991
$Q_m = 56.6$ m <sup>3</sup> /s ( $U = 9.3$ m/s)								
$A_r$ [ $10^{-10}$ m/s]	7.75	2.51	5.64	0.65	0.47	0.36	0.20	0.47
$A_d$ [mm/year]	5.56	1.8	3.96	0.47	0.34	0.26	0.14	0.33
$Q_{pl} = 68.0$ m <sup>3</sup> /s ( $U = 11.3$ m/s)								
$A_r$ [ $10^{-10}$ m/s]	7.66	2.73	5.28	0.64	0.47	0.39	0.22	0.44
$A_d$ [mm/year]	5.49	2.00	1.6	0.46	0.33	0.28	0.16	0.32
mean of both operating scenarios								
$A_r$ [ $10^{-10}$ m/s]	7.71	2.62	5.4	0.65	0.47	0.38	0.21	0.45
<b><math>A_d</math> [mm/year]</b>	<b>5.53</b>	<b>1.90</b>	<b>3.96</b>	<b>0.47</b>	<b>0.34</b>	<b>0.27</b>	<b>0.15</b>	<b>0.33</b>

\* values scaled by factor 12 due to calibration with Pfaffensprung data

Additionally, the adapted Ishibashi model (Auel *et al.* 2016b), neglecting the second term in Eq. (1), was applied for the granite lining of Pfaffensprung SBT using the coefficient  $C_l$  for concrete as no values are available for bedrock materials. It was found that the model overestimates the measured abrasion by 12 times (compare column 4 with 9 in Table 2). Hence, the constant  $C_l$  was adjusted by applying the abrasion data of the granite at Pfaffensprung SBT resulting in  $C_l = 9.91 \times 10^{-9} \approx 10^{-8}$  [m<sup>2</sup>/(kgf)], which lies between concrete ( $\sim 10^{-7}$  [m<sup>2</sup>/(kgf)]) and steel ( $\sim 10^{-11}$  [m<sup>2</sup>/(kgf)]). The adjusted  $C_l$  was used for the abrasion estimate for Hardy Island Granite at Mud Mountain SBT (last column in Table 2). Despite the calibration and reasonable abrasion estimation as com-

pared to the Auel and Sklar and Dietrich models (Table 2), the Ishibashi model is not recommended for the use to estimate abrasion of rock (such as granite) as it was developed for concrete and steel only.

The annual abrasion depths of Mud Mountain SBT for both operation scenarios (last row in Table 2) varied from  $A_d = 0.34$  mm/year (average) to 0.47 mm/year (severe) using Auel's model and from  $A_d = 0.15$  mm/year (average) to  $A_d = 0.27$  mm/year (severe) using the Sklar and Dietrich model. The latter model showed lower abrasion depths compared to the Auel model, which is attributed to the application range of the models. The Sklar and Dietrich model is applied for bedrock incision in rivers where flow is subcritical and the bed is rough while Auel's model covers sub- to highly supercritical flow conditions and various bed configurations from planar to alluvial. Therefore, as a conservative estimate, the annual average depth of 0.47 mm/year or 0.26 mm per 10,000 tons/m of bed load (per unit tunnel width) might be expected. This estimate is also supported by the results obtained at Pfaffensprung SBT in Switzerland (Müller-Hagmann 2017). Despite higher annual average abrasion depths of 2.9 mm/year, its rate per 10,000 tons/m of bed load was 0.26 mm and hence is the same as for Mud Mountain SBT. Although the granite for Mud Mountain SBT is stronger than the one at Pfaffensprung SBT (223 vs. 180 MPa), the different hydraulic conditions result in the same abrasion depth per 10,000 tons/m of bed load rate.

The average abrasion depths for the mean of both operation scenarios (mean discharge and pool limit discharge) at Mud Mountain SBT are plotted versus the number of operation years (Figure 3). Three lines are plotted accounting for the hydrologic variability. For each abrasion model, the solid lines are for the long-term average sediment transport rate of 49,500 tons/year, while the dashed lines refer to an intense (+62%) and a light (-62%) sediment transport rate, representing wet and dry years, respectively. The results show a linear increase of the abrasion depths  $h_a$  with time of SBT. The results from the Auel and the Ishibashi models are similar here, whereas the Sklar and Dietrich model gives lower values as explained above.

For long-term abrasion prediction, that is over decades, a spatially averaged annual abrasion depth of  $0.47 \approx 0.50$  mm/year  $\pm 85\%$  (estimation error resulting from uncertainty of  $k_v$  calculation at Pfaffensprung; Müller-Hagmann 2017) for average sediment transport and  $0.47 \times 1.62 = 0.76 \approx 0.80$  mm/year  $\pm 85\%$  for intense sediment transport conditions, respectively, should be considered as a conservative approach.

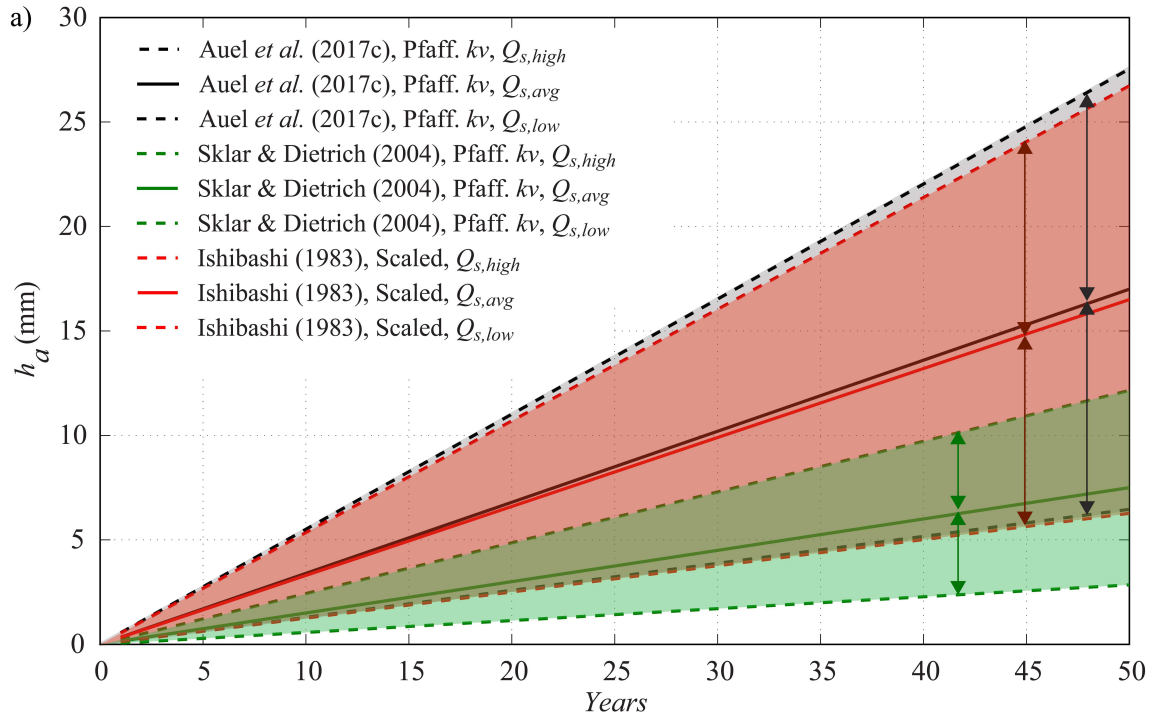


Figure 3: Estimated spatially averaged abrasion depths of Mud Mountain SBT invert lined with Hardy Island Granite versus years of tunnel operation for average abrasion conditions. Sediment load entering the tunnel is  $Q_s = 49,500$  tons/year. Dashed lines correspond to  $\pm 62\%$  of  $Q_s$ . Annual abrasion depths obtained from different models are listed in Table 2.

## 5 Conclusions

This paper briefly describes three different abrasion prediction models and their applications for the granite invert lining at Mud Mountain SBT, Washington, USA. The different abrasion models are calibrated based on the abrasion measurement data acquired at the granite test fields in the Pfaffensprung SBT, Switzerland. The calibrated models are applied to Mud Mountain SBT for two operating scenarios to predict spatially averaged abrasion depths as function of time and sediment load. The estimated annual spatially averaged abrasion depths for Hardy Island Granite are approx. 0.50 mm/year for average and 0.80 mm/year for intense sediment transport conditions, respectively. However, local abrasion depths occurring at edges and joints of the granite blocks might be considerably higher than the spatially averaged values.

## Acknowledgement

The authors would like to thank the US Army Corps of Engineers, Seattle District, for allowing us to present the analysis of Mud Mountain 9-foot Tunnel.

## References

Annandale, G. (2013). Quenching the thirst. Sustainable water supply and climate change. CreateSpace Independent Publishing Platform, North Charleston, USA.

- Auel, C., Kobayashi, S., Sumi, T., Takemon, Y. (2017a). Effects of sediment bypass tunnels on sediment grain size distribution and benthic habitats. *River Sedimentation* (Wieprecht *et al.* eds.), Taylor and Francis Group, London: 825–832.
- Auel, C., Albayrak, I., Sumi, T., Boes, R.M. (2017b). Sediment transport in high-speed flows over a fixed bed: 1. Particle dynamics. *Earth Surface Processes and Landforms*, DOI: 10.1002/esp.4128.
- Auel, C., Albayrak, I., Sumi, T., Boes, R.M. (2017c). Sediment transport in high-speed flows over a fixed bed: 2. Particle impacts and abrasion prediction. *Earth Surface Processes and Landforms*, DOI: 10.1002/esp.4132.
- Auel, C., Kantoush, S.A., Sumi, T. (2016a). Positive effects of reservoir sedimentation management on reservoir life: Examples from Japan. *84<sup>th</sup> Annual Meeting of ICOLD*, Johannesburg, South Africa 4-11–4-20.
- Auel, C., Boes, R.M., Sumi, T. (2016b). Invert abrasion prediction at Asahi sediment bypass tunnel, Japan. *Journal of Applied Water Engineering and Research* DOI: 10.1080/23249676.2016.1265470.
- Auel, C., Boes, R. (2011). Sediment bypass tunnel design – review and outlook. *Proc. ICOLD Symposium - Dams under changing challenges* (Schleiss & Boes, Eds.), 79<sup>th</sup> Annual Meeting of ICOLD, Lucerne, Switzerland. Taylor & Francis, London, UK: 403–412.
- Baumer, A., Radogna, R. (2015). Rehabilitation of the Palagnedra sediment bypass tunnel (2011-2013). *Proc. 1. Int. Workshop on Sediment Bypass Tunnels*, VAW Mitteilungen 232 (R. Boes, ed.), ETH Zurich, Switzerland: 235–245.
- Beer, A.R., Turowski, J.M. (2015). Bedload transport controls bedrock erosion under sediment-starved conditions. *Earth Surface Dynamics* 3: 291–309.
- Bitter, J.G.A. (1963a). A study of erosion phenomena, part I. *Wear* (6): 5–21.
- Bitter, J.G.A. (1963b). A study of erosion phenomena, part II. *Wear* (6): 169–190.
- Boes, R.M., Auel, C., Haggmann, M., Albayrak, I. (2014). Sediment bypass tunnels to mitigate reservoir sedimentation and restore sediment continuity. *Reservoir Sedimentation* (Schleiss *et al.*, Eds.), Taylor & Francis Group, London, UK: 221–228.
- Czuba, J. A., Magirl, C. S., Czuba, C. R., Curran, C. A., Johnson, K. H., Olsen, T. D., Kimball, H. K., Gish, C. C. (2012). Geomorphic analysis of the river response to sedimentation downstream of Mount Rainier, Washington. U.S. Geological Survey Open-File Report 2012-1242, 134 p.
- Facchini, M., Siviglia, A., Boes, R.M. (2015). Downstream morphological impact of a sediment bypass tunnel – preliminary results and forthcoming actions. *Proc. 1st Int. Workshop on Sediment Bypass Tunnels*, ETH Zurich, VAW Mitteilungen 232 (Boes, Ed.): 137-146.
- Fukuda, T., Yamashita, K., Osada, K., Fukuoka, S. (2012). Study on flushing mechanism of dam reservoir sedimentation and recovery of riffle-pool in downstream reach by a flushing bypass tunnel. *Proc. Intl. Symposium on Dams for a changing world*, Kyoto, Japan.
- Helbig, U., Horlacher, H.-B. (2007). Ein Approximationsverfahren zur rechnerischen Bestimmung des Hydroabrasionsverschleißes an überströmten Betonoberflächen (A approximation method for the determination of hydroabrasive wear on overflowed concrete surfaces). *Bautechnik* 84(12): 854–861 (in German).
- ICOLD (2009). Sedimentation and sustainable use of reservoirs and river systems. *Bulletin 147*, International Commission on Large Dams, Paris, France.

- Ishibashi, T. (1983). Hydraulic study on protection for erosion of sediment flush equipments of dams. *Civil Society Proc.* 334(6): 103–112 (in Japanese).
- Jacobs, F., Winkler, K., Hunkeler, F., Volkart, P. (2001). Betonabrasion im Wasserbau (Concrete abrasion in hydraulic structures). *VAW Mitteilungen* 168 (Minor HE, ed.), ETH Zurich, Switzerland (in German).
- Kondolf, G.M., Gao, Y., Annandale, G.W., Morris, G.L., Jiang, E., Zhang, J., Carling, P., Fu, K., Guo, Q., Hotchkiss, R., Peteuil, C., Sumi, T., Wang, H.-W., Wang, Z., Wei, Z., Wu, B., Yang, C.T. (2014). Sustainable sediment management in reservoirs and regulated rivers: Experiences from five continents. *Earth's Future* 2(5): 256-280.
- Lamb, M.P., Dietrich, W.E., Sklar, L.S. (2008). A model for fluvial bedrock incision by impacting suspended and bed load sediment. *Journal of Geophysical Research: Earth Surface* 113(F03025).
- Martín, E.J., Doering, M., Robinson, C.T. (2015). Ecological effects of sediment bypass tunnels. *Proc. 1st Int. Workshop on Sediment Bypass Tunnels*, ETH Zurich, VAW Mitteilungen 232 (Boes, Ed.): 147-156.
- Morris, G.L., Fan, J. (1998). Reservoir sedimentation handbook. McGraw-Hill Book Co., New York, USA.
- Müller-Hagmann, M. (2017). Hydroabrasion in high-speed flows at sediment bypass tunnels. *PhD Thesis, VAW-Mitteilungen* 239 (R. Boes ed.), ETH Zurich, Switzerland.
- Schleiss, A., Oehy, C. (2002). Verlandung von Stauseen und Nachhaltigkeit (Sedimentation of reservoir and sustainability). *Wasser, Energie, Luft* 94(7/8): 227–234 (in German).
- Sklar, L.S., Dietrich, W.E. (2004). A mechanistic model for river incision into bedrock by saltating bed load. *Water Resources Research* 40(W06301).
- Sklar, L.S., Dietrich, W.E. (1998). River longitudinal profiles and bedrock incision models: Stream power and the influence of sediment supply. Rivers over rock: Fluvial processes in bedrock channels (eds. Winkler KJ, Wohl EE). *Geophysical Monograph Series* 107: 237–260.
- Sumi, T., Okano, M., Takata, Y. (2004). Reservoir sedimentation management with bypass tunnels in Japan. *Proc. 9<sup>th</sup> International Symposium on River Sedimentation*, Yichang, China: 1036–1043.
- Turowski, J.M. (2012). Semi-alluvial channels and sediment-flux-driven bedrock erosion. *Gravel-Bed Rivers: Processes, Tools, Environments* (eds. M. Church, P. M. Biron and A. G. Roy), John Wiley & Sons, Ltd, Chichester, UK.
- Turowski, J.M. (2009). Stochastic modeling of the cover effect and bedrock erosion. *Water Resources Research* 45(W03422).
- USACE (2016). Mud Mountain Dam 9-Foot Tunnel Rearmoring, Enumclaw, WA - Construction Solicitation and Specifications, Phase 2 of 2. *US Army Corps of Engineers*, RFP No. W912DW-16-R-0006.
- VAW (2016). Mud Mountain Dam 9-foot Tunnel Re-armoring: Abrasion Calculations and Recommendations on the Invert Lining Concept - Expertise report. *VAW Report 4357*, Laboratory of Hydraulics, Hydrology and Glaciology, ETH Zurich, Switzerland.
- Whipple, K.X., Hancock, G.S., Anderson, R.S. (2000). River incision into bedrock: Mechanics and relative efficacy of plucking, abrasion and cavitation. *Geological Society of America Bulletin* 112(3): 490–503.

## **Authors**

Christian Auel (corresponding Author)

John R. Thene

ILF Consulting Engineers, Rum/Innsbruck, Austria

Michelle Müller-Hagmann

Ismail Albayrak

Robert M. Boes

Laboratory of Hydraulics, Hydrology and Glaciology, ETH Zurich, Switzerland

Email: [christian.uel@alumni.ethz.ch](mailto:christian.uel@alumni.ethz.ch)